

Kinetics of CO Oxidation Over $\text{Co}_3\text{O}_4/\gamma\text{-Al}_2\text{O}_3$

Part I: Steady State

Steady state experiments and their interpretation were performed to explore the kinetics of CO oxidation over a supported Co_3O_4 catalyst. The rate of reaction was found to depend on temperature and the partial pressure of oxygen but not on the partial pressure of carbon monoxide. It is shown that catalyst dynamics must be accounted for to achieve real understanding.

DEEPAK PERTI

and R. L. KABEL

Department of Chemical Engineering
Pennsylvania State University
University Park, PA 16802

SCOPE

Among the transition metal oxides, cobalt oxide (Co_3O_4) is one of the most active catalysts for carbon monoxide oxidation. The catalytic surface is known to play an important role, yet there is no consensus in the literature regarding the reaction mechanism. The only previous extensive study of this reaction system was by Yao (1974), who emphasized the comparison of activities of cobalt oxide catalysts prepared by various methods. She showed that the catalytic activity of Co_3O_4 for CO oxidation could even compare favorably with the noble metals, but her rate data were not sufficiently definitive to attempt any mechanistic interpretations. The broad goal of the three papers

that comprise this series is to elucidate the mechanistic character of oxidation-reduction catalysis by metal oxides. This first paper deals with conventional steady state experimentation. A fixed-bed reactor was used to study the dependence of conversion (and thence reaction rate) on flow rate, temperature, CO and O_2 partial pressures, and catalyst characteristics. The interpretation of the steady state results enhances understanding, but more importantly it establishes a basis for comparison of the results of the dynamic studies described in Parts II and III.

CONCLUSIONS AND SIGNIFICANCE

The experiments under constant reactor conditions of temperature, feed rate, and feed composition demonstrated that the state of the catalyst was being altered even during steady reaction conditions. This was most dramatically evidenced by a long-term, reversible decline in activity but also in more subtle ways. By experimental design and data manipulation, conversion data were adjusted to a common level of catalytic activity. Steady state interpretation of the resulting data yielded the rate equation

$$r_o = 3.9 \times 10^9 e^{-1.27 \times 10^5 / RT} P_{\text{O}_2}^{0.412}$$

This equation is similar to the result of Yao except for the lack of dependence on carbon monoxide partial pressure. The observed dependence on P_{O_2} suggests that the slowest step in the overall reaction is the reoxidation of a surface site, previously depleted in oxygen by reaction with carbon monoxide. Clearly, however, more discriminating experiments are required. These are provided by the reactor dynamics studies described in the following paper (Part II).

INTRODUCTION

Among metal oxides, those of the 3-d transition metals are generally active catalysts for CO and hydrocarbon oxidation. Past

studies have revealed that Co_3O_4 is a more active catalyst for these reactions than are the other 3-d metal oxides (Yao, 1975; Dwyer, 1972; Shelef et al., 1968; Hofer et al., 1964; Katz et al., 1975; Krylov, 1970; Borekov, 1973). Its activity has been found to be comparable to that of the noble metals, such as Pt and Pd.

In spite of its proven superiority, supported Co_3O_4 has not been a subject of detailed kinetic study for CO or hydrocarbon oxidation. Most previous work emphasizes the comparison of catalytic ac-

Deepak Perti is currently with E. I. duPont de Nemours and Company, Photo Systems and Electronic Products Department, Wilmington, DE 19898.
Correspondence concerning this paper should be addressed to R. L. Kabel

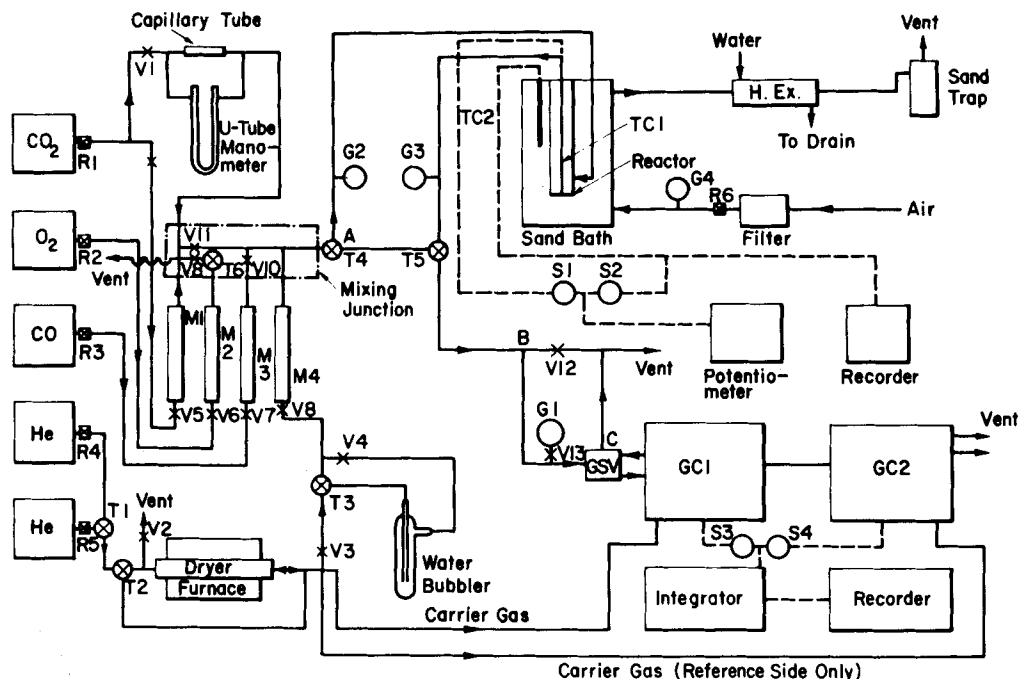


Figure 1. Schematic diagram of the equipment.

R	= high pressure gas regulators	GSV	= gas sampling valve
M	= rotameters	GC	= gas chromatograph
V	= valves	TC	= thermocouple
T	= three-way valves	H.Ex	= heat exchanger
G	= pressure gages		

activities of various oxide catalysts, including Co_3O_4 . Even the work done by Yao (1974), which deals exclusively with unsupported and supported Co_3O_4 , concentrates on the comparison of catalytic activities of cobalt oxide catalysts prepared by different methods.

Yao found that the low temperature (≈ 473 K) reaction rate for CO oxidation over supported or unsupported catalysts could be represented in a power law form, $\text{rate} = k P_{\text{O}_2}^m P_{\text{CO}}^n P_{\text{H}_2\text{O}}^{-l} e^{-E/RT}$, with m , n , and l in the range of 0.3 to 0.5. Activation energies of 6.3 and 8.3×10^4 J/mol were reported for supported and pure Co_3O_4 , respectively. These results give an excellent picture of the comparative activities of the various catalysts, but the mode of data treatment suggests that the kinetic results for any one catalyst are first approximations at best. Yao did not attempt to deduce a reaction mechanism from these results.

Several other works qualitatively describe the possible reaction mechanism for CO oxidation over Co_3O_4 and the other metal oxides (Dwyer, 1972; Hofer et al., 1964; Krylov, 1970; Boreskov, 1973; Klissurski et al., 1970; Hertl, 1973). However, there is a dearth of quantitative treatment on this subject. This paper presents conventional steady state experiments and data analysis in an attempt to narrow this gap.

EXPERIMENT

Catalyst

The supported catalyst $\text{Co}_3\text{O}_4/\gamma\text{-Al}_2\text{O}_3$ was prepared by an impregnation technique. Pellets of $\gamma\text{-Al}_2\text{O}_3$ (1.6×1.6 mm) were soaked in cobalt nitrate solution, filtered, and calcined at 773 K for 4 h. The Co_3O_4 loading was 6.851 g Co_3O_4 /100 g $\gamma\text{-Al}_2\text{O}_3$. This was determined by comparing weights of the catalyst and pure support pellets at 523 K and 4.0 Pa. The BET area of both the support and the supported catalyst was 250 m^2/g . Analysis of x-ray diffraction patterns showed only Co_3O_4 and $\gamma\text{-Al}_2\text{O}_3$ phases. Electron microprobe and scanning electron microscope x-ray mapping techniques revealed a well-dispersed Co_3O_4 phase at 0.1 μm resolution. Further details on the catalyst can be found in Perti (1980).

Equipment

A vertical, stainless steel 316, fixed-bed reactor (16.8 mm I.D.) was used. The reactor tube was 0.5 m long and had an axial thermowell (2.7 mm O.D.) with a sliding thermocouple. Alternate layers of glass beads and catalyst (6.345 g cat. total) were used. There were 11 layers of catalyst, each 3.81 mm thick. The lowest layer was 0.128 m above the bottom of the reactor tube. The portions of the reactor tube, above and below the layered catalyst bed, were also filled with glass beads. The reactor tube was maintained isothermal by a fluidized sand bath made out of a 0.12 m I.D. steel tube, clad with heating mantles. Temperature was controlled manually by simultaneous adjustments of the voltage supplied to the heating mantles, and the air pressure used to fluidize the sand bath. Finer control was obtained by adjusting the voltage supplied to a cartridge heater immersed horizontally at the bottom of the sand bath. In the absence of reaction, axial and radial temperature control within the reaction zone was better than ± 0.25 K. Control within ± 0.5 K was achieved in all steady state experiments. Even in the most severe cases (the transient experiments, reported in Part II) temperatures were controlled with ± 1 K.

Research grade O_2 , CO, and He were used to produce the reaction mixture. The feed composition was established by setting the flow rate of each gas as measured by rotameters. The reactor pressure was monitored by a pressure gauge at the reactor outlet and was controlled by a fine metering valve with a micrometer head. The effluent from the reactor was analyzed by bleeding a part of the stream through two gas chromatographic columns in series. The first column (6.35 mm O.D. and 0.61 m long) contained silica gel at 320 K and separated CO_2 from CO and O_2 . The second column (6.35 mm O.D. and 1.524 m long) had molecular sieve 13X at 298 K and separated O_2 from CO. The entire separation was achieved in less than 4 min. Helium, used both as a diluent in the feed and as the carrier gas to the chromatographs, did not interfere with the analysis. A digital integrator was used to analyze the chromatographic data. The details of the equipment and the method of chromatographic data analysis can be found elsewhere (Perti, 1980). A schematic layout of the equipment is shown in Figure 1.

Nature of Experiments Performed

The determination of reaction rate in steady state fixed-bed reactors is

guided by the plug-flow reactor mass balance, which for carbon monoxide is

$$r dW = F_{CO} dx_{CO} \quad (1)$$

The rate of reaction, r , is based on the mass of catalyst. Solving Eq. 1 for r gives

$$r = \frac{dx_{CO}}{d(W/F_{CO})} \quad (2)$$

Equation 2 demonstrates the convenience of direct interpretation of x_{CO} vs. W/F_{CO} data.

To minimize heat and mass transfer effects and to approximate a differential reactor, conversion for each run was kept below 5%. At any particular set of partial pressures of CO and O₂, P_{CO} and P_{O_2} , various runs were conducted to determine x_{CO} at different values of W/F_{CO} . The mass of catalyst, W , was constant throughout the steady state experimental program. Variation of W/F_{CO} was achieved by independent adjustments of the flow rates of O₂, CO, and He from run to run such that F_{CO} could be varied without altering P_{CO} and P_{O_2} . The procedure was repeated for various sets of P_{CO} and P_{O_2} . The effect of temperature was ascertained by studying one particular set of values for P_{CO} and P_{O_2} at different temperatures.

RESULTS AND DISCUSSION

Catalyst Deactivation and Regeneration

Fresh catalyst, after being heated in air at 563 K for 4 days, was exposed at 488.6 K to a reaction mixture in which $P_{CO} = 2.3$ kPa and $P_{O_2} = 2.0$ kPa. The volumetric flow rate given in Figure 2 corresponds to $W/F_{CO} = 254.7$ g(cat) h/mol. These conditions comprised the standard run. Figure 2 shows that after a brief initial increase the conversion steadily drops over 8 days to almost 50% of its original level.

After the data shown in Figure 2 were obtained, the catalyst was subjected to repeated regenerations in air and periods when the partial pressures of CO and O₂ were twice their standard run values. Standard runs were interspersed regularly among these treatments. It was found that all observed changes in catalyst activity were fully reversible.

During the eight-day period in which the standard run conversions were monitored for the fresh catalyst (Figure 2), several runs at different values of W/F_{CO} were conducted. These runs were conducted at the same partial pressures of CO and O₂ as those for the standard run. The results are shown in Figure 3. The x_{CO} vs. W/F_{CO} data can be separated into three distinct curves, each corresponding to a different time period during which the data were collected. The shift in the curves is toward lower conversions for data obtained when the reactor had been on stream for longer periods of time. Among the data in Figure 3 are some of the stan-

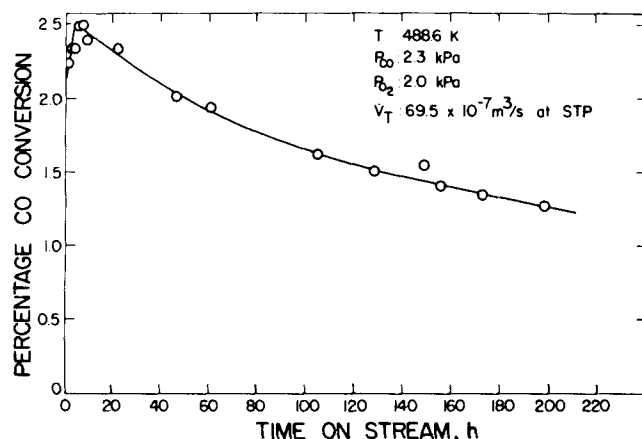


Figure 2. Change in the catalytic activity at the standard run conditions.

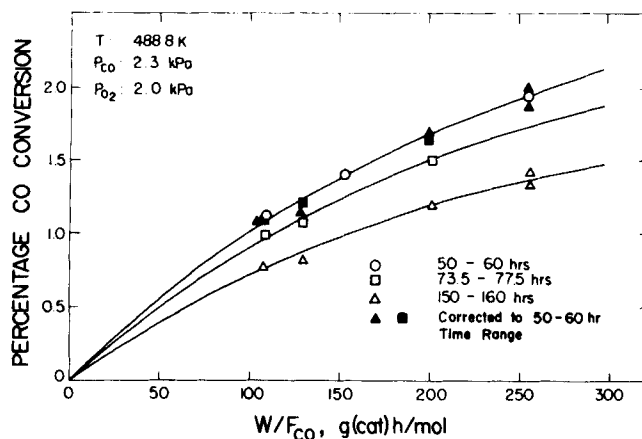


Figure 3. Compensation for reversible catalyst deactivation.

dard run data that were monitored throughout the time period ($W/F_{CO} = 254.7$ g(cat) h/mol).

A simple relationship was found to be quite effective in correcting all conversion data to a common level of catalytic activity. The initial standard run activity is dependent on the extent of "regeneration" as well as the state of the catalyst prior to the regeneration. However, it was found that an experimentally convenient, overnight regeneration in pure oxygen following a day's worth of experiments was able to return the initial standard run conversion to $1.95 \pm 0.1\%$. It was, therefore, decided to select 1.95% as the reference standard run conversion. From Figure 2 or 3, this value can be seen to correspond closely to the 50-60 h time period of the top curve in Figure 3.

The standard run conversion at any time can be obtained from the line through the data of Figure 2. Multiplying the observed conversion at any time by the ratio of 1.95 to the standard run percent conversion for the same time normalizes the experimental conversion data to a common activity level, as shown in Figure 3. The corrected values of all the conversions in the lower two curves of Figure 3 are replotted as solid symbols and are seen to follow closely the upper curve. In the experiments of any given day the catalyst deactivation was small and only minor corrections were required. The runs at the other partial pressures were interspersed with runs at the standard run conditions and a procedure similar to that illustrated above was used to find the corrected conversion values. This approach is reminiscent of that advocated by Sinfelt (1968). The rest of the conversion values reported in this paper are corrected.

Although catalyst deactivation was not the focus of this research, there is much to be learned from our observations. The phenomenon of very high initial catalyst activity compared to some eventual steady state activity is common but seldom studied because of the commercial importance and greater ease of study of stable catalysts. We believe that the continuation of our experiment for more than one week would have led to a steady state activity level. However, the ease of return to a state of common catalyst activity enabled us to work in this more active, and scientifically interesting, region.

The reversibility of the decline rules out catalyst decay by sintering. Deactivation caused by coking is also unlikely because the temperature of regeneration is not high enough to burn off any carbon that might have been deposited by a reaction of type $2CO \rightarrow C + CO_2$. The deactivation is probably caused by some kind of slow blocking or depletion of the active sites on the surface. A second deactivation phenomenon will be introduced shortly.

The observed decay in catalyst activity means that the steady state of which we speak in the title and throughout this paper is illusory. What we have done is to manipulate our data to reflect

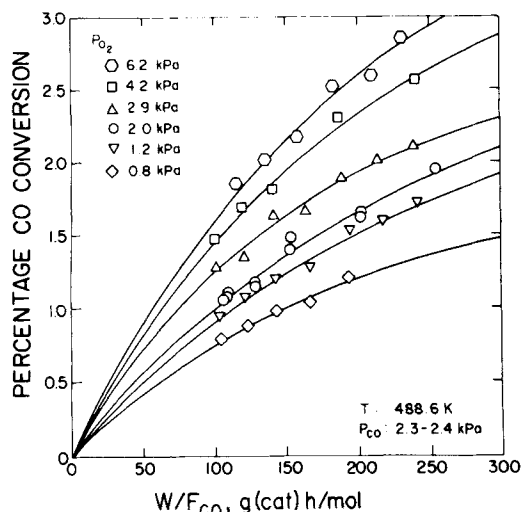


Figure 4. Effect of P_{O_2} on conversion.

the circumstances at a point in time, thus simulating a steady state that does not really exist. This familiar approach is informative, as will be seen, but it is clear that ultimately a dynamic interpretation will be more fruitful still.

Effect of P_{O_2} on Initial Reaction Rate

To ascertain the effect of oxygen on the reaction rate, six sets of experiments were performed at $P_{CO} = 2.35 \pm 0.05$ kPa and P_{O_2} ranging from 0.8 to 6.2 kPa. The results are shown in Figure 4. If the reactor behaves differentially, i.e., partial pressures do not change significantly during the passage of the reaction mixture through the reactor, a plot of x_{CO} vs. W/F_{CO} should yield a straight line, according to Eq. 2. However, the results in Figure 4 show consistent curvature and possible bias, i.e., a tendency to intersect the vertical axis above the origin. These features are evident also in data to be presented later in Figures 6 and 7.

The possible bias could be caused by errors in gas chromatograph or flow meter calibrations. Time after time these calibrations were shown to be valid. A detailed error analysis suggests a maximal error of ± 0.1 in the value of the parameter plotted on the ordinate. By inspection of the figures, this magnitude can be seen to be consistent with the observed scatter in the data.

The observed curvature could mean that internal or external heat and mass transfer effects are disguising the reaction rate, that the reactor is not acting differentially, or that the plug-flow assumption is not valid, i.e., there is some axial dispersion and/or a lack of perfect radial mixing in the reactor. The strong observed temperature dependence (see later) suggests that physical processes are not limiting the reaction process. Unfortunately, the small reactor diameter required to assure isothermality and the size of the $\gamma\text{-Al}_2\text{O}_3$ extrudate available for catalyst preparation precluded experimental verification of the absence of mass transfer resistances by the variation of particle size. To ascertain whether internal and external heat and mass transfer are affecting the reaction rate, various criteria given in the literature were evaluated by using the observed rates of reaction and other experimental conditions. The method used to obtain the reaction rate is described later, as are crucial reaction parameters, such as activation energy and the reaction orders.

The following criterion, developed by Mears (1971a), was used to evaluate the effect of intraparticle (internal) heat and mass transfer on the reaction rates:

$$\frac{\tau_{OBS} \tau_p^2}{C_s D_e} |n - \gamma \beta| < 1 \quad (3)$$

This criterion was found to be satisfied for the most stringent case, i.e., where D_e is the smallest and τ_{OBS}/C_s is the largest.

Effects of external interphase heat and mass transfer were evaluated by calculating the overall effectiveness factor defined by Carberry (1976)

$$\bar{\eta} = (1 - \bar{\eta} Da)^n \exp \left[-\gamma \left\{ \frac{1}{1 + \beta \bar{\eta} Da} - 1 \right\} \right] \quad (4)$$

A value of $\bar{\eta}$ close to unity indicates that the interphase heat and mass transfer effects do not disguise the observed reaction rates. A value of $\bar{\eta} = 1.0042$ was obtained corresponding to the most stringent case, i.e., the lowest total flow rate used in this work.

Mears (1971a,b) found that among the intrareactor or interparticle heat and mass transfer effects, radial heat transfer affects the reaction rate more strongly than the others. He developed the following criterion, which if fulfilled, assures less than 5% influence of radial interparticle heat transfer on the reaction rate:

$$|\Delta H| \tau_{OBS} r_t^2 / k_e T_w < [1 + 8 (r_p/r_t) Bi_w] \quad (5)$$

The above criterion was also found to be satisfied for the conditions used in this work.

Mears (1971a) has suggested that to assure negligible axial dispersion effects for non-first-order reactions obeying a power law form, the following criterion should be satisfied:

$$\frac{L}{D_p} > \frac{20n}{P_{ea}} \ln \frac{C_0^0}{C_f} \quad (6)$$

At a conversion of 33%, the right-hand side of the above expression becomes equal to L/D_p for each catalyst layer used in the packed bed. Thus, at the 5% or lower conversion levels obtained in this work, axial dispersion effects can be ignored.

Thus, in the absence of radial mass transfer resistance and axial dispersion, the plug-flow assumption seems to be a valid one. Keeping conversion values below 5% also virtually assures a differential reactor, especially because the effect of CO_2 on the reaction rate was found to be minimal (Perti, 1980).

It should be made clear that all of these criteria apply only to steady state. They do not guarantee that the corresponding features will be unimportant in the interpretation of transient phenomena in Part II.

The cause for the curvature in x_{CO} vs. W/F_{CO} (Figure 4) remains unclear. The presence of the thermowell within the packed bed could contribute to this behavior. More likely the effect is chemical, due to an altered state of the catalyst at higher conversion values. More will be said on the latter effect at the end of this paper.

Whatever the cause of the nonlinearity in the x_{CO} vs. W/F_{CO} curve may be, the reaction rate can be obtained by taking the slope of the curve provided the plug-flow assumption holds. The slope is the steepest at the origin and can be called the initial reaction rate or the reaction rate at the inlet to the reactor because W/F_{CO} approaches zero as W does. Whatever small influence CO_2 has on the reaction rate will not be observed at the inlet to the reactor. Moreover, the reactant partial pressures are known at the inlet (feed conditions) to the reactor.

Data differentiation, especially with extrapolation, can amplify errors substantially. Accordingly, we used a variety of analytical fitting functions as well as purely graphical methods to obtain initial rates. All gave comparable results. Among the functions was Eq. 7, which was derived (lengthy and approximate) by inserting a power function rate equation into Eq. 1 and integrating.

$$x_{CO} = A(1 - e^{-B W/F_{CO}}) \quad (7)$$

Equation 7 was found to fit the integral data excellently as well as to pass through the origin. A nonlinear least-squares regression technique was used to find the values of the lumped constants, A and B , in Eq. 7, which gave the best fit to the data. The fit is shown

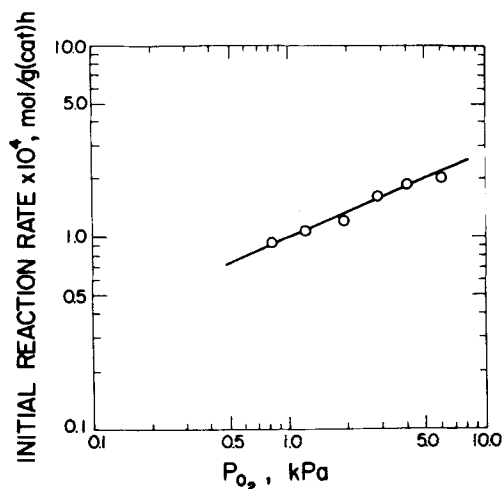


Figure 5. Reaction order with respect to oxygen.

by the solid lines in Figure 4, as well as in Figure 7.

The initial rates of reaction, obtained by analytical differentiation of Eq. 7, are plotted logarithmically in Figure 5 as a function of P_{O_2} . The linearity of the data is excellent, as indicated by a correlation index of 0.968. This correlation suggests a power law form of rate expression. The reaction order with respect to oxygen was found to be 0.412 by measuring the slope of the straight line in Figure 5.

Effect of P_{CO} on the Initial Reaction Rate

To obtain the effect of carbon monoxide on the reaction rate, six sets of experimental runs were conducted at a constant P_{O_2} of 2.0 kPa and P_{CO} ranging from 1.6 to 4.5 kPa. The results are plotted in Figure 6. The most obvious conclusion is that one curve can adequately fit all of the data, unlike the case where P_{O_2} was varied at a constant P_{CO} (Figure 4). Scrutiny of the six individual data sets may hint at minor CO influence. Since one curve fits all of the data, the rate of reaction must be virtually independent of the CO partial pressure.

To confirm the unexpected result described above, three more data sets were obtained at the different, but also constant, P_{O_2} level of 4.2 kPa. First, sets of P_{CO} of 1.05 and 2.4 kPa were run. Later, the set at $P_{CO} = 2.4$ kPa was repeated to check for reproducibility. These x_{CO} vs. W/F_{CO} data are also plotted in Figure 6. Once again it can be seen that one curve fits all of the data satisfactorily. There is no indication of CO influence in this case. This reaffirms the observation that the P_{CO} does not influence the reaction rate.

Effect of Temperature on the Initial Reaction Rate

The effect of temperature on the initial reaction rate was determined by conducting experiments at 498.4 and 508.2 K to supplement the data obtained at 488.6 K. The P_{CO} and P_{O_2} were kept constant at 2.3 and 2.0 kPa, respectively, for all three temperatures.

The method used for correcting to the standard run reference conversion was different in these sets. In the oxygen and carbon monoxide partial pressure studies, the temperature was kept constant at 488.6 K and the standard run was also conducted at that temperature. If the same standard run were to be used for studies at different temperatures, the temperature would need to be changed every time a standard run is conducted. This was found to be very time consuming, as much time was required to achieve a new steady state following a temperature change of 10 K.

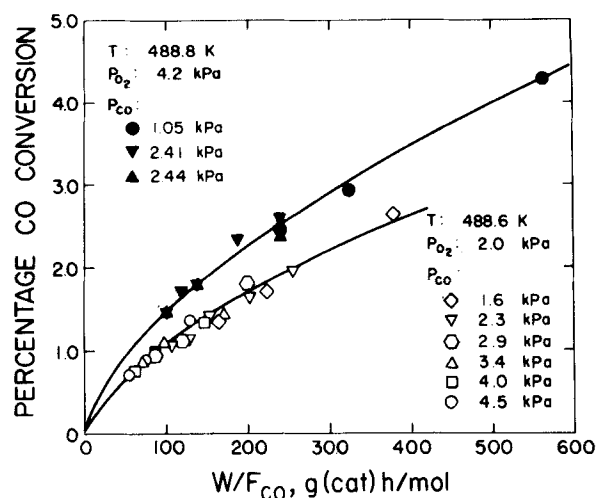


Figure 6. Results of CO partial pressure studies.

This problem was circumvented by redefining the standard run. The "regeneration" was carried out at a low oxygen flow rate of 3.33×10^{-7} m³/s for 16 to 20 h prior to the runs at any temperature. At 488.6 K, runs at $P_{CO} = 2.3$ kPa and $P_{O_2} = 2.0$ kPa conducted 3 to 4 h after such regeneration were found to give 1.95% conversion, the same as the reference standard run conversion at 488.6 K. The first runs at 498.4 and 508.2 K, taken 3 to 4 h after the same regeneration were designated as the standard run for the corresponding temperature sets. The standard run was repeated twice or three times during the period in which that set was performed. The other conversion values were corrected following the procedure described earlier. Such a procedure assumes that similar regenerations at different temperatures would bring the catalyst to a comparable state. The possible impact of this assumption is addressed shortly.

The x_{CO} vs. W/F_{CO} data at different temperatures are shown in Figure 7. The shapes of x_{CO} vs. W/F_{CO} curves are similar at all three temperatures. The initial reaction rates were obtained by finding the slopes at the origin of the regressed curves. These initial reaction rates are plotted semilogarithmically against the reciprocal temperature in Figure 8. The resulting good linear fit indicates the suitability of the Arrhenius equation for the correlation of the initial reaction rates with temperature.

The activation energy and the frequency factor were found from the slope and intercept of Figure 8 to be 1.273×10^5 J/mol and 3.913×10^9 mol/g(cat)h(kPa)^{0.412}, respectively.

EMPIRICAL RATE EXPRESSION

On the basis of the experimental findings and discussions presented earlier, the initial rate of reaction can be expressed as

$$r_o = 3.9 \times 10^9 e^{-1.273 \times 10^5 / RT} P_{O_2}^{0.412} \quad (8)$$

in the temperature range of 488 to 508 K. The absolute values of the initial rate are based on a catalytic activity level that is easily reproducible by an overnight regeneration in oxygen at the temperature of interest. Prolonged use of the catalyst under reaction conditions results in a decay in the catalytic activity. Thus, for extended periods between regenerations, lower initial rates of reaction than predicted by Eq. 8 would be observed.

A comparison of the above rate expression can be made with the results of Yao (1974), the only other available results in the literature for CO oxidation over supported cobalt oxide. Yao has reported the following rate expression:

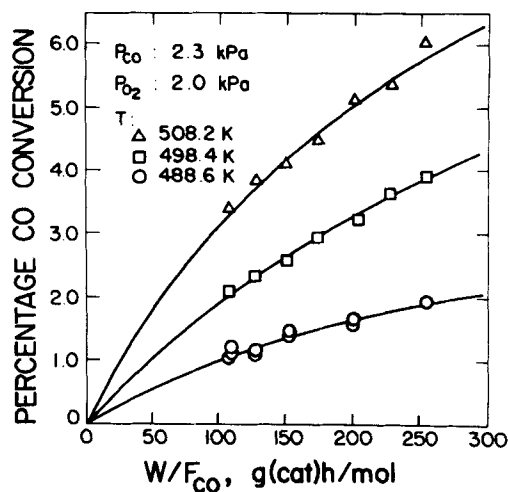


Figure 7. Influence of temperature on conversion.

$$r = A e^{-6.3 \times 10^4 / RT} P_{O_2}^{0.44} P_{CO}^{0.47} \quad (9)$$

in the temperature range of 398–473 K. Equation 9 is for a variety of supported catalysts prepared at 873 K, with somewhat lower orders and activation energy appearing for catalysts prepared at 1123 K. Yao used γ - and α -alumina obtained from different sources and prepared the catalyst by impregnation in $Co(NO_3)_2$, by impregnation followed by treatment in NH_3 , and directly by mechanical mixing.

Yao found specific values of the reaction rate at 473 K for the different catalysts to vary by orders of magnitude. Quantitative comparisons of rates determined by Yao and in this work are unwarranted because of significant differences in the supports and methods of preparation of the catalysts. Suffice it to note that the rates in this and her work are of similar magnitude for the most comparable catalysts.

The activation energy obtained in this work is almost twice that reported by Yao for supported Co_3O_4 . The present value 1.273×10^5 J/mol is also in the upper range of reported values for CO oxidation over metal oxide catalysts. A high activation energy implies that the rate of reaction is very sensitive to temperature. Such an effect could have been artificially produced by the definition of the standard run used earlier to correct for the effect of the decay in catalytic activity. The standard run was chosen to be different at different temperatures with the assumption that a similar catalyst pretreatment at any temperature would yield an identical catalytic state. More likely the same regeneration pretreatment at a higher temperature would make the catalyst more active. This would cause the activation energy calculated in this work to be higher than its actual value.

The order of reaction with respect to oxygen in this work agrees closely with Yao's. The most striking difference between the results of this work and Yao's is the fact that the dependencies on P_{CO} are different. In her paper, Yao has not mentioned the method she used to determine the reaction rate. She realized the importance and difficulty in approaching the conditions of a differential reactor. Therefore she only used the results obtained at less than 30% conversion. For correlational purposes, she assumed the partial pressure of the reactants to be the average of the inlet and the outlet values. It is common practice in catalysis research to presume a differential reactor and to use the linear approximation to Eq. 2, $r = x_{CO}/(W/F_{CO})$, without checking the integral data for linearity. In view of the experimental results found in this work and what is known about Yao's methods, it seems very unlikely that her reactor was truly differential. Perti (1980) has shown that it is possible to obtain a false indication of P_{CO} dependency in the rate of reaction if in-

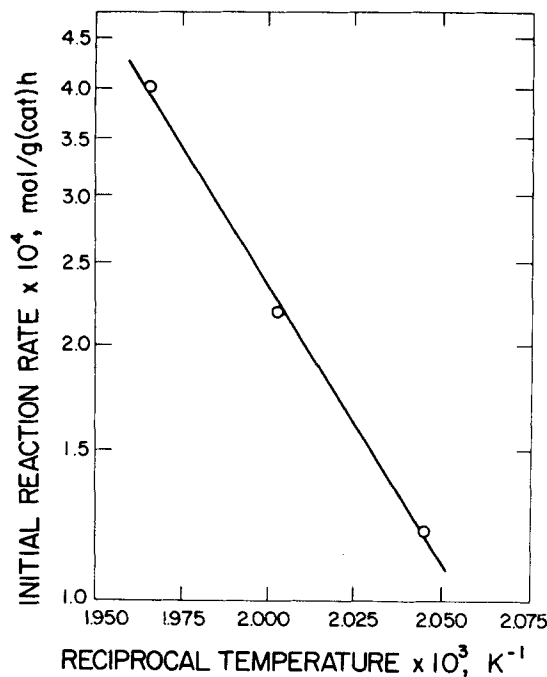


Figure 8. Arrhenius plot.

tegral data are analyzed on the incorrect assumption that the reactor is differential.

FURTHER INTERPRETATION

Returning to the issues of curvature and possible bias in the integral data, we can now consider whether these would have any impact on the conclusions from the steady state studies. Obviously the minimal dependence on CO is not affected by these issues. Also, whether straight or curved lines, intersecting the ordinate above the origin, are placed through the data, one still obtains a fractional order for oxygen. Rather than to attribute these observed behaviors to some obscure experimental error, it seems wiser to look for chemical explanations.

An explanation for the curvature and apparent bias of the integral data may reside in the imperfection of the mass of catalyst as a quantitative measure of the number of active sites. Operating in this very active regime may cause the number of active sites to be sensitive to the conversion level, even though product poisoning appears not to be the case. One could imagine that higher conversion levels could diminish the number (or accessibility) of active sites, causing the observed conversion to be less than proportional to the mass of catalyst, W . Further, it is reasonable that the curvature resulting from such a mechanism would be greatest at the lowest level of conversion. This is a form of deactivation with a different basis than that observed in Figure 2. Qualitative evidence for both forms of deactivation is put forth in Part III.

Some direct measure of the active sites, such as was performed in a different reaction system by Kabel and Johanson (1962), would be desirable. But the task is more difficult for metal oxide catalysts than for ion exchange resins or supported metal catalysts, for which titration by chemisorption has become quite common. Yao and Shelef (1974) performed selective chemisorption of CO and NO on Co_3O_4 . The NO adsorption studies went smoothly, but the CO studies were complicated by reaction. In particular, they postulated both irreversible and reversible CO adsorption. We believe the latter was actually irreversible adsorption of CO followed by desorption of unidentified reaction product, CO_2 . Reversible CO

adsorption is in conflict with the findings of Hertl (1973) and the reactor dynamics portion of this work. It is shown in Parts II and III that there are three kinds of sites and three kinds of oxygen involved in this catalytic reaction system. Thus simple titration of sites is not likely to be definitive. The dynamic method of Hsu and Kabel (1974) should be especially suitable for exploring the concomitant rate processes taking place. Real understanding requires a mastery of the catalyst dynamics.

SEARCH FOR A REACTION MECHANISM

The traditional approach to obtaining a reaction mechanism is to propose a series of elementary reaction steps. Each proposed mechanism is simplified on the basis of a single rate-determining step, quasi-equilibrium, and/or steady state approximation until a rate expression can be reached that has a form close to the obtained empirical form (power law, Langmuir-Hinshelwood, etc.) or that can otherwise fit the steady state kinetic data. The empirical rate equation, obtained in the steady state studies, indicates that the initial rate depends only on P_{O_2} . While this strongly indicates that an elementary step involving a surface site and gaseous oxygen is the slowest (or rate-determining step), it does not provide information as to what the other steps might be.

CO oxidation over metal oxides is generally thought to proceed via an oxidation-reduction mechanism where CO reacts with a surface oxygen and forms an adsorbed carbonate species, which subsequently desorbs as CO_2 . The surface site, now depleted in oxygen, is then regenerated by reaction with oxygen from the gas phase. If this last step is assumed to be the rate-determining step, many possible sequences for the remaining steps can be written. When simplified, such sequences yield a rate expression similar to the obtained power law form, Eq. 8, with the order of oxygen equal to 0.5.

It is evident that more discriminating experiments are needed to elucidate further mechanistic details. Dynamic studies in the existing reactor offer the opportunity to obtain much new kinetic information in the identical environment used for the steady state studies. The results from an extensive series of unsteady state experiments, which are described in Parts II and III, substantiate and augment those that have been presented here.

ACKNOWLEDGMENT

The authors wish to acknowledge the effective collaboration of Paul I. Hodgen and Gregory J. McCarthy. Financial aid was provided by the National Science Foundation, Exxon Education Fund, E. I. duPont de Nemours & Company, and Union Carbide Corporation. Their assistance is appreciated.

NOTATION

Bi_w	= Biot number at the reactor wall
C_f	= final or outlet concentration, $\text{mol}\cdot\text{m}^{-3}$
C_o	= initial or inlet concentration, $\text{mol}\cdot\text{m}^{-3}$
C_s	= surface concentration, $\text{mol}\cdot\text{m}^{-3}$
Da	= Damkohler number
D_e	= effective diffusivity within the catalyst particle, $\text{m}^2\cdot\text{s}^{-1}$
D_p	= diameter of the catalyst particle, m
E	= activation energy, $\text{J}\cdot\text{mol}^{-1}$
F_{CO}	= feed rate of CO, $\text{mol}\cdot\text{h}^{-1}$
ΔH	= heat of reaction, $\text{J}\cdot\text{mol}^{-1}$
k	= rate constant
k_e	= effective thermal conductivity of the packed bed, $\text{W}\cdot\text{m}^{-1}\cdot\text{K}^{-1}$

l	= reaction order
L	= reactor length, m
m	= reaction order
n	= reaction order
P_{CO}, P_{O_2}	= partial pressure of the subscripted species, kPa
Pe_a	= axial Peclet number
r	= reaction rate of CO, $\text{mol}\cdot\text{g}(\text{cat})^{-1}\cdot\text{h}^{-1}$
r_o	= initial reaction rate of CO, $\text{mol}\cdot\text{g}(\text{cat})^{-1}\cdot\text{h}^{-1}$
r_{OBS}	= observed reaction rate, $\text{mol}\cdot\text{g}(\text{cat})^{-1}\cdot\text{h}^{-1}$
r_p	= particle radius, m
r_t	= reactor tube radius, m
R	= universal gas constant
T	= temperature, K
T_w	= wall temperature, K
\dot{V}_T	= total volumetric flow rate, $\text{m}^3\cdot\text{s}^{-1}$
W	= weight of the catalyst, g
x_{CO}	= fractional conversion of carbon monoxide

Greek Letters

β	= internal Prater number
$\bar{\beta}$	= external Prater number
γ	= Arrhenius factor
$\bar{\eta}$	= overall interphase effectiveness factor

LITERATURE CITED

- Boreskov, G. K., "Mechanism of Catalytic Oxidation Reactions on Solid Oxide Catalysts," *Kin. Kat.*, **14**, 7 (1973).
- Carberry, J. J., *Chemical and Catalytic Reaction Engineering*, McGraw-Hill, New York (1976).
- Dwyer, F. G., "Catalysis for Control of Automotive Emissions," *Catal. Rev.*, **6**, 261 (1972).
- Hertl, W., "Infrared Spectroscopic Study of Catalytic Oxidation Reactions Over Cobalt Oxide Under Steady State Conditions," *J. Catal.*, **31**, 231 (1973).
- Hofer, L. T. E., P. Gussey, and R. B. Anderson, "Specificity of Catalysts for the Oxidation of Carbon Monoxide-Ethylene Mixtures," *J. Catal.*, **3**, 451 (1964).
- Hsu, S. M., and R. L. Kabel, "A Batch Reactor to Study Concomitant Adsorption and Heterogeneous Catalysis," *J. Catal.*, **33**, 74 (1974).
- Kabel, R. L., and L. N. Johanson, "Reaction Kinetics and Adsorption Equilibria in the Vapor-Phase Dehydration of Ethanol," *AIChE J.*, **8**, 621 (1962).
- Katz, S., J. J. Croat, and J. V. Laukonis, "Lanthanum Lead Manganite Catalyst for Carbon Monoxide and Propylene Oxidation," *Ind. Eng. Chem. Prod. Res. Dev.*, **14**, 274 (1975).
- Klissurski, D., et al., "Catalytic Oxidation of Carbon Monoxide of Co_3O_4 ," *Khim. Ind. (Sofia)*, **57**, 293 (1970).
- Krylov, O. V., in *Catalysis by Non-Metals*, Academic Press, New York (1970).
- Mears, D. E., "Tests for Transport Limitations in Experimental Catalytic Reactors," *Ind. Eng. Chem. Proc. Des. Dev.*, **10**, 541 (1971a).
- , "Diagnostic Criteria for Heat Transport Limitations in Fixed Bed Reactors," *J. Catal.*, **20**, 127 (1971b).
- Perti, D., "Kinetics of Carbon Monoxide Oxidation Over Supported Cobalt Oxide Catalyst," Ph.D. Thesis, Pennsylvania State University (1980).
- Shelef, M., K. Otto, and H. Gandhi, "The Oxidation of CO by O_2 and NO on Supported Chromium Oxide and Other Metal Oxide Catalysts," *J. Catal.*, **12**, 361 (1968).
- Sinfelt, J. H., "A Simple Experimental Method for Catalytic Kinetic Studies," *Chem. Eng. Sci.*, **23**, 1181 (1968).
- Yao, H. C., and M. Shelef, "Nitric Oxide and Carbon Monoxide Chemisorption on Cobalt-Containing Spinel," *J. Phys. Chem.*, **78**, 2490 (1974).
- Yao, Y.-F. Y., "The Oxidation of Hydrocarbons and CO over Metal Oxides. III. Co_3O_4 ," *J. Catal.*, **33**, 108 (1974).
- , "The Oxidation of CO and C_2H_4 over Metal Oxides. V. SO_2 Effects," *J. Catal.*, **39**, 104 (1975).

Manuscript received Oct. 2, 1981; revision received Nov. 18, 1982 and accepted Aug. 17, 1984.